ELSEVIER

Ceramics International 25 (1999) 511–516

CERAMICS INTERNATIONAL

Interaction of mullite with some polluting oxides in diesel vehicle filters

Maria Teresa Dario, Alessandro Bachiorrini*

Dipartimento di Scienze e Tecnologie Chimiche, Università di Udine, Via del Cotonificio, 108, 33100 Udine, Italy

Received 1 July 1997; accepted 26 August 1997

Abstract

Mullite is one of the most promising substitutes for cordierite as a material for the manufacture of diesel vehicle filters. This study investigated the sensitivity of mullite to chemical attack provoked by some of the oxides present in the particulate of diesel-engine exhaust gases. Filter thermal regeneration conditions were simulated by means of heat treatments between 400 and 1000°C. The following pollutants were used: V_2O_5, PbO, ZnO, Fe_2O_3, CeO_2, $CaCO_3$ and Na_2CO_3 (the last-mentioned as oxide generators). The results obtained were compared with those for cordierite. Mullite was less sensitive to attack than cordierite but was unable to effectively resist attack by PbO and Na_2CO_3.

1. Introduction

For about 20 years, diesel-engine vehicles have been fitted with cordierite honeycomb filters for the purpose of limiting atmospheric pollution. These filters have, however, proved to have a relatively short useful life. Recent studies have shown that damage to the cordierite structure is a result of: (a) continuously alternating dimensional variations due to the operational thermal cycles of the vehicle [1] and (b) chemical interactions taking place between oxides present in exhaust gas particulate and cordierite [2,3] at temperatures below those the filter may reach during thermal regeneration cycles (>1000°C) [4]. It has been shown that only iron and cerium oxides, out of all those present in exhaust-gas particulate, are chemically inert [3,5] for cordierite whereas ZnO, CaO, V_2O_5, PbO and Na_2CO_3 react by solid–state diffusion at 1000, 900, 750, 550 and 500°C, respectively. In particular, Na_2CO_3, which is formed by oxide conversion in the presence of air, reacts with cordierite by means of a complex mechanism [6] to provoke more significant destructive effects than those produced by other reagent oxides. It has also been ascertained that the action of sodium is intensified by synergy in the presence of other oxides in the particulate, especially V_2O_5 [7].

For some time, proposals have been made for a number of alternative filter materials [8–18]. Mullite, ZrO_2, TiO_2, α or γ Al_2O_3, SiC and Al_2TiO_5 are some of the most frequently mentioned candidates but sillimanite, petalite, sialon, Si_3N_4 and BN have also been suggested. Finally, some recent studies have aimed at the realisation of porous fibre-reinforced structures [9] based on mixtures of refractory ceramic powders. Mullite is one of the most promising substitute materials. The aim of this study was to verify the resistance of mullite to chemical attack caused by particulate oxides during filter regeneration cycles. The results were subsequently compared with those obtained for cordierite.

2. Experimental

2.1. Materials and methods

The following commercially-available products were used to simulate the most aggressive components of exhaust particulate: $CaCO_3$ (Fisher), Na_2CO_3, ZnO, CeO_2, V_2O_5 and PbO (all Aldrich 99 + %), Fe_2O_3 (Selenia). Carbonates were employed as sources for the corresponding oxides partly in order to avoid problems related to their high reactivity to CO_2 in the atmosphere and partly because both sodium and calcium are present as carbonates in diesel exhaust particulate. Mullite was prepared by sol–gel following a small–scale version of

* Corresponding author.

0272-8842/99/$ - see front matter
PII: S0272-8842(97)00086-2

the procedure of Yoldas [20,21] modified as described hereunder. A total of 22 mmol of distilled water was added drop by drop to a solution of ethyl alcohol (EtOH Baker; 815 mmol) and tetraethyl orthosilicate ($Si(OEt)_4$ Aldrich 99 + %, 17.8 mmol) at a thermostat-controlled temperature of 60°C, and stirred. After an interval of about 10 min, aluminium tri-*sec*-butoxide ($Al(O-secBut)_3$ Aldrich 97%, 53 mmol) was added quickly to produce partial hydrolysis of the alcoholate. The solution turned milk-white and then within 5 min became transparent. Hydrolytic condensation was induced by adding HCl (Baker 36–38%; 1.43 mmol) diluted with water (47.2 mmol) and ethanol (318 mmol) together while continuing to agitate the solution. Si–O–Al bonding was indicated by increasing opalescence and temporary gelation of the mixture. After 20 min the reaction was completed by the slow addition (1 drop every 30 min) of a solution of water (72 mmol) and EtOH (348 mmol). Permanent gelation was observed at the end of the procedure.

The product was oven-dried at 70°C (24 h) and calcinated at 400°C for 2 h before being characterised by IR analysis.

At this stage, the powder was an amorphous phase which on further heating crystallised directly into mullite with an exothermic process at about 980°C observed by DTA. In order to ensure that crystallisation of the amorphous phase was complete, a final heat treatment of 3 h at 1450°C was performed.

One–to–one (by weight) mixtures were prepared of crystalline mullite and each of the oxides used to simulate the conditions created at the particulate–ceramic filter interface. Mixing was carried out by wet mechanical grinding (isopropanol for 1 h). After drying at 70°C, a series of pellets ($\varnothing = 12.7$ mm) was obtained for each mixture by pressing uniaxially a weighed amount (200 mg) of powder at 400 MPa. Each compact was placed in a platinum crucible and heated to a selected maximum temperature in a programmable oven ((Neztsch) (heating rate: 10°C min^{-1}, isotherm at final temperature for 5 min). Maximum temperatures set ranged from 400°C (to simulate normal filter operating conditions) to 1000°C (the assumed minimum limit reached during filter regeneration cycles). After this treatment, each specimen was quenched to room temperature under vacuum in a desiccator.

2.2. Analysis

All samples were crushed to powder and analysed by X-ray diffractometry (XRD) and Fourier Transform Infrared (FTIR) analysis.

XRD spectra were acquired on powder samples using monochromatic $CoK_{\alpha 1}$ radiation from an INEL XRG 3000 instrument (acquisition time 30 min). FTIR analyses were carried out on sample pellets dispersed in KBr using an OMNIC program-controlled NICOLET Magna-IR550 interferometer with resolution set at 4 cm^{-1}.

3. Results and discussion

XRD examination revealed that in the cases of the mullite–$CaCO_3$, mullite–ZnO, mullite–Fe_2O_3, mullite–CeO_2 and mullite–V_2O_5 mixtures, there were no phases due to chemical reaction even at 1000°C. In contrast, the mullite–Na_2CO_3 and mullite–PbO mixtures revealed the formation of new crystalline phases as a result of heat treatment-induced chemical interaction. Data obtained from XRD examination of the last two mixtures is given in Table 1. Fig. 1 illustrates the FTIR spectra of materials used to prepare the mixtures. Figs. 2 and 3 detail the most significant FTIR spectra of the heat–treated mixtures.

3.1. Interaction with Na_2CO_3

The XRD analyses (Table 1) indicate that the first crystalline product deriving from the chemical interaction of mullite and sodium carbonate, an aluminosilicate of sodium ($NaAlSiO_4$), was formed at 750°C. Since the Al/Si ratio in this product is 1/1 whereas in mullite it is 3/1, it may be deduced that the missing aluminum is in the amorphous phase. The corresponding FTIR spectrum (Fig. 2, curve 2) shows an increase in diffusion and a decrease in resolution of IR bands that is characteristic of amorphous or disordered crystalline substances. The second possibility can be excluded because the XRD diffractograms display no broadenings or shifts of the diffraction peaks. IR band diffusion is therefore indicative of the presence of an amorphous phase in the sample.

The higher the heat-treatment temperature, the greater the intensity of the $NaAlSiO_4$ diffractometer peaks. Mullite and carbonate diffractometer peaks, in contrast, lose intensity as the temperature rises. Mullite can be considered to have reacted almost completely at 900°C.[1] The XRD for this sample show, in addition to $NaAlSiO_4$, another entirely silicate crystalline phase: γ-$Na_2Si_2O_5$. Since no other aluminum–containing component is identifiable (with aluminum as a silicate, sodium aluminate or other form), we deduce that excess Al deriving from the reaction of mullite with sodium is present in the amorphous phase.

[1] The presence of mullite in the sample heat-treated at 900 and 1000°C cannot be clearly inferred from the XR diffractograms firstly because the peaks have poor intensity and blend into the background and secondly because they partially overlap with the γ–$Na_2Si_2O_5$ peaks. In addition, the FTIR spectra enable us to exclude the presence of mullite at 1000°C since the characteristic pair of bands at 1160 and 1130 cm^{-1} is absent.

Table 1
Phases identified by XRD analysis. Numbers in brackets indicate intensity ratio of characteristic peak and average background values of diffractogram

Temperature (°c)	Mullite–Na_2CO_3 mixture		Mullite-PbO mixture	
25	$Al_6Si_2O_{13}$(5.8)	Na_2CO_3(4.7)	$Al_6Si_2O_{13}$(2.3)	PbO(28.2)
400	$Al_6Si_2O_{13}$(5.7)	Na_2CO_3(4.2)	$Al_6Si_2O_{13}$(2.5) αPbO_2(4.5)	PbO(8.1)
500			$Al_6Si_2O_{13}$(2.4) αPbO_2(6.4)	PbO(8.6)
600	$Al_6Si_2O_{13}$(5.7)	Na_2CO_3(4.7)	$Al_6Si_2O_{13}$(2.0) αPbO_2(4.9)	PbO(14.2)
700	$Al_6Si_2O_{13}$(5.4)	Na_2CO_3(4.7)	$Al_6Si_2O_{13}$(2.9)	PbO(39.0)
750	$Al_6Si_2O_{13}$(5.2) $NaAlSiO_4$(18)	Na_2CO_3(4.5)		
800	$Al_6Si_2O_{13}$(14.6) $NaAlSiO_4$(3.2)	Na_2CO_{13}(4.0)	$Al_6Si_2O_{13}$(2.1) $PbAl_2O_4$(4.7) [b]	PbO(27.9)
900	$Al_6Si_2O_{13}$(1.9)[a] $NaAlSiO_4$(8.6)	Na_2CO_3(2.9) γ-$Na_2Si_2O_5$(17.4)	$Al_6Si_2O_{13}$(1.9) αPbO_2(4.6) $Pb_3SiAl_{10}O_{20}$(1.8) Pb_4SiO_6(3.3) [b]	$PbO_{1.55}$(2.0) $PbAl_2O_4$(3.3) Pb_2SiO_4(2.2) $Pb_3Si_2O_7$(2.2)
1000	$Al_6Si_2O_{13}$(1.4)[a] $NaAlSiO_4$(6.7)	Na_2CO_3(2.4) γ-$Na_2Si_2O_5$(10.6)	$Al_6Si_2O_{16}$(1.4) Pb_2O_3(4.3)	$Pb_3SiAl_{10}O_{20}$(4.3)

[a] Attribution uncertain owing to overlapping of a secondary γ $Na_2Si_2O_5$ peak and characteristic mullite peak, and to high background/peak ratio.
[b] Diffractograms with very high background and diffuse peaks.

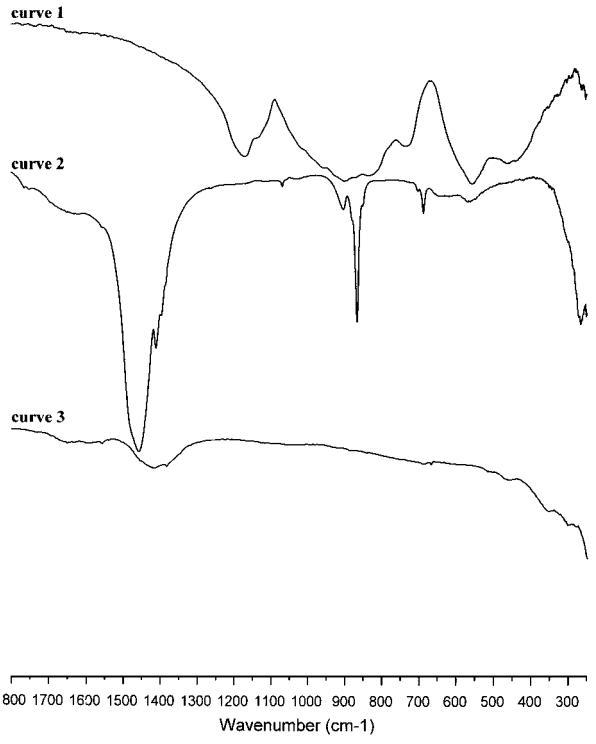

Fig. 1. FTIR spectra of: mullite (curve 1), Na_2CO_3 (curve 2) and PbO (curve 3).

A new phase at 750°C is confirmed from FTIR analysis by the appearance of a new band at about 443 cm^{-1} (Fig. 2, curve 2). At higher temperatures, this band increases, as therefore does the new phase. The shoulder at about 650 cm^{-1} in the spectrum at 750°C becomes a pair of diffuse bands (at about 650 and 620 cm^{-1}).

The FTIR spectrum of the sample heat-treated at 900°C (Fig. 2, curve 4) shows no evidence of absorption bands deriving from the γ-$Na_2Si_2O_5$ identified by XRD analysis.

The absence of FTIR absorption bands in the range 1200–1150 cm^{-1} denotes both the disappearance of mullite and the lack of SiO_4 group with four Si–O–Si bridges whose characteristic asymmetric stretching absorption occur in this region [19]. The latter evidence, together with the fact that the diffractometric peaks of sodium silicate display a marked broadening, enables us to deduce that the phase is distorted.

Moreover, the absence of asymmetric SiO_4 group stretching bands with four Si–O–Si bridges implies that the corresponding symmetric mode is also absent. The absorptions between 740 and 540 are not therefore attributable to γ-$Na_2Si_2O_5$. Bending of these SiO_4 groups contributes instead to absorption in the zone between 520 and 470 cm^{-1} [22].

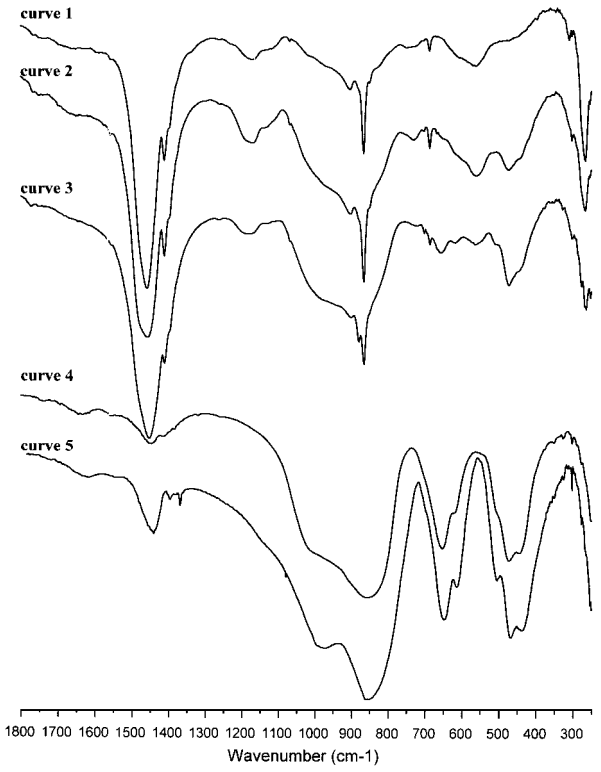

Fig. 2. FTIR spectra of mullite–Na_2CO_3 mixture heat-treated at: 700°C (curve 1), 750°C (curve 2), 800°C (curve 3), 900°C (curve 4) and 1000°C (curve 5).

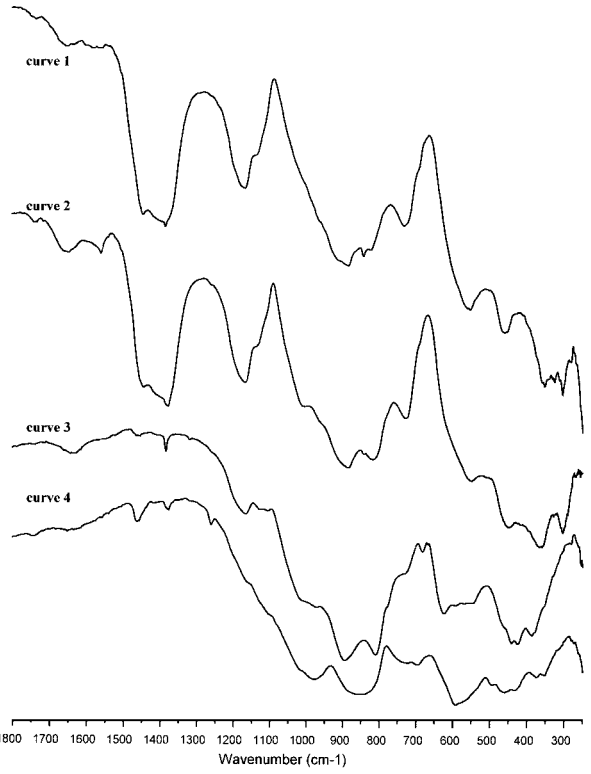

Fig. 3. FTIR spectra of mullite–PbO mixture heat-treated at: 600°C (curve 1), 800°C (curve 2), 900°C (curve 3) and 1000°C (curve 4).

On comparing the spectra of tests at 800 and 900°C (Fig. 2, curves 3 and 4, respectively), it will be noted that the 650 cm^{-1} band undergoes a substantial increase in intensity, becoming comparable to the band at 473 cm^{-1}. Since both bands are attributable to $NaAlSiO_4$, it may be deduced that a new phase is contributing to absorption at 650 cm^{-1}. It is probable that this phase is the amorphous $NaAlO_2$ the spectrum of a crystalline sample of which is reported in Fig. 4 (curve 1).

The FTIR spectrum of the sample treated at 1000°C (Fig. 2, curve 5) presents no substantial variations except that the absorption peaks already present at 900°C now have better definition.

Cordierite tested in the same way with sodium carbonate [3] is already seriously attacked at 600°C (with formation of $Na_2Al_2SiO_6$) and at 800°C it undergoes complete degradation and is transformed into other phases.

From a comparison of the attack onset temperatures, it emerges that mullite, although unstable in the presence of sodium, is in all cases more durable than cordierite.

3.2. Interaction with PbO

FTIR (Fig. 3) and XRD (Table 1) analysis of samples treated below 800°C highlight variations deriving from oxidation of lead oxide, which readily absorbs atmospheric CO_2 to form the corresponding carbonate.

In the XRD spectrum of the sample heat-treated at 800°C, there are traces of $PbAl_2O_4$ but not of silicates or aluminosilicates. This result may be explained if we consider that the silicate liberated by the reaction of the attack on the mullite is stabilised by excess lead as a glassy phase. More rapid quenching than that adopted in the present study would be required to maintain an aluminate in the amorphous phase.

The FTIR spectrum of the sample treated at 800°C (Fig. 3,curve 2) fails to confirm the presence of lead aluminate firstly because only a modest quantity is present and secondly because the bands typical of $PbAl_2O_4$ (Fig. 4,curve 2) absorb in the same spectrum region as mullite and the lead oxides. The onset of attack is indicated in the spectrophotometric examination only by the appearance of the FTIR shoulder at about 1010 cm^{-1} (attributable to stretching of SiO lattice-end bonds) and the shift of frequencies corresponding to the AlO_4 (ν_s from 890 to 885 cm^{-1};δ_{as} from 735 to 730 cm^{-1}) and AlO_6 (ν_s from 555 to 550 cm^{-1}; δ_{as} from 830 to 820 cm^{-1}) groups.

At 900°C, XRD analysis reveals a further increase in the amorphous phase and the formation of small quantities of lead aluminum silicate ($Pb_3SiAl_{10}O_{20}$) and silicates of lead (Pb_2SiO_4, Pb_4SiO_6, $Pb_3Si_2O_7$) as well as the continuing presence of $PbAl_2O_4$. The corresponding FTIR spectrum (Fig. 3, curve 3) shows significant differences with respect to preceding spectra as new

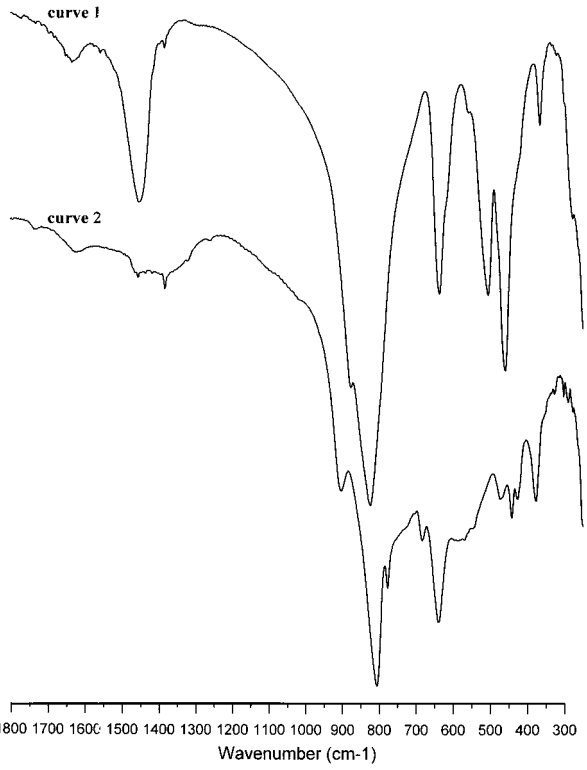

Fig. 4. FTIR spectra of: $\gamma NaAlO_2$ (curve 1) and $PbAl_2O_4$ (curve 2).

bands have appeared at 1104, 780, 682, 624 and 591 cm^{-1} while bands already present in previous test spectra have undergone a shift. Moreover the broadening of the bands confirms an increase in the amorphous phase. It was not possible to attribute bands to the individual phases identified by diffractometric analysis because of the complexity of the spectrum, which was mainly due to the considerable reciprocal interference by the spectra of individual phases. The presence of mullite is, however, certain since its characteristic band with a maximum of 1165 cm^{-1} is evident. At 1000°C, the sample largely comprised an amorphous phase. The diffractogram displays a very high background and relatively broadened peaks, as does the FTIR spectrum (Fig. 3, curve 4). Mullite and Pb_2O_3 are present only as low crystallised residues, the fraction of $Pb_3SiAl_{10}O_{20}$ has increased and lead silicates has completely disappeared.

PbO therefore attacks mullite, beginning to interact at 800°C (Table 1) and producing almost total disintegration after only 5 min at 1000°C.

Cordierite subjected to the same tests with lead oxide [3] begins to react at 600°C to form Pb_2SiO_4 and at 900°C has been totally destroyed and transformed into other phases. As in the case of sodium carbonate, so too with lead oxide mullite displays greater stability than cordierite even though it begins to be attacked at temperatures markedly lower than those reached during thermal regeneration cycles.

3.3. Thermochemical behaviour of mullite–V_2O_5, mullite–CeO_2, mullite–Fe_2O_3, mullite–$CaCO_3$ and mullite–ZnO mixtures

On comparing the XRD spectra of the mullite–V_2O_5 mixture heat–treated to 700°C against that of the untreated mixture, no variations are observed. In contrast at temperatures equal to or greater than 750°C, only an increase in the background attributable to amorphous V_2O_5 can be seen (M.p. = 690°C). Similar behaviour is observable in the FTIR spectra where, beginning at 750°C, diffusion of the V_2O_5 bands may be noted, indicating that this oxide is present as amorphous phase.

Similar tests conducted on cordierite [3] showed that V_2O_5 began to attack at 800°C, forming SiO_2 and MgV_2O_6 but did not lead to complete disintegration even after prolonged heating at 1000°C (50 h) [7].

The XRD spectra of the mullite–CeO_2 mixture heat-treated to 1000°C and that of the untreated mixture are practically identical, as are the FTIR spectra. This behaviour is entirely analogous to the behaviour of cordierite, which proved not to interact thermochemically with cerium oxide [5].

There is also an absence of heat treatment-induced interactions in the case of the mullite–Fe_2O_3 mixture since both the XRD and FTIR spectra of tests carried out up to 1000°C practically overlap the corresponding spectra for the nonheat-treated mixture. Here again mullite behaves in a similar fashion to cordierite [3], which is not attacked by iron oxide.

Diffractometric and spectrophotometric analyses of the heat-treatment tests carried out with the mullite–$CaCO_3$ mixture failed to reveal any chemical interaction between the components even at 1000°C. The differences found in the XRD and FTIR spectra above 750°C are due to the thermal decomposition of $CaCO_3$ into the corresponding oxide.

In contrast at 900°C, cordierite begins to be attacked by CaO to form melitite [3].

On the basis of the XRD and FTIR analyses, there is no evidence of any interaction in the case of the mullite-ZnO mixtures even after heat treatment at 1000°C. Here too mullite displays greater stability than cordierite, which at 1000°C interacts with zinc oxide to form Zn_2SiO_4 and $MgAl_2O_4$.

4. Conclusions

Data collected during this study enable us to affirm that mullite is more resistant than cordierite to chemical attacks provoked by the oxides in diesel-engine particulate. Mullite does not interact with the oxides of Ca, Zn or V, all of which are able to degrade cordierite filters. It is attacked by the oxides of Na and Pb at

temperatures which are higher than those observed in the case of cordierite.

It should be pointed out that the interaction of mullite with PbO and NaO takes place at temperatures lower than those reached by the filter during thermal regeneration cycles and that the absence of any chemical interaction does not preclude that a mullite filter might be damaged nevertheless.

Oxides with fusion temperatures lower than those reached by the filter (as is the case of V_2O_5 M.p. = 690°C and PbO M.p. = 888°C) may melt into the filter pores and block them.

In assessing the suitability of mullite with respect to cordierite, it must also be remembered that the commercially-available product, unlike the synthetic variety used in this study, will contain impurities (metal cations) that could facilitate chemical attack.

References

[1] S. Maschio, C. Schimid, E. Lucchini, S. Roitti, A. Gandini, Atti del Congresso Omaggio Scientifico a Renato Turriziani, Vol. 2 Rome, 22–24 April 1992, pp. 2.541–2.552.
[2] A. Negro, L. Montanaro, P.P. Demaestri, A. Giachello, A. Bachiorrini, J. Eur. Ceram. Soc. 12 (1993) 493–498.
[3] L. Montanaro, A. Bachiorrini, A. Negro, J. Eur. Ceram. Soc. 13 (1994) 129–134.
[4] A. Giachello, P.P. Demaestri, G. De Portu, S. Guicciardi, Proc. CIMTEC, World Ceramic Congress, Montecatini, 24–30 June 1990.
[5] A. Montorsi, R. Delorenzo, E. Verné, Ceram. Int. 20 (1994) 353–358.
[6] A. Bachiorrini, Ceram. Int. 22 (1996) 73–77.
[7] L. Montanaro, A. Bachiorrini, Ceram. Int. 20 (1994) 169–174.
[8] H.G. Nitzsche, H. Kessel, Haus Tech., Essen, Vortragsveroff, 206 (1969) 70–79.
[9] R.D. Bagley, R.C. Doman, D.A. Duke, R.N. Mcnally, SAE Tech. Pap. 730274, 1973.
[10] I.M. Kolesnikov, I.N. Frolova, Zh. Prikl. Khim. (Leningrad), 55 (1982) 561–571.
[11] F.J. Sergeys, US patent no. 3 926 851, 16 December 1975.
[12] Y. Takenchi, German patent no. 2 411 222, 12 August 1976.
[13] J. Nemeth, US patent no. 4 040 998, 9 August 1997.
[14] T.Nakamura, Jpn. Tokyo Koho patent no. 78 121 010, 12 October 1978.
[15] K. Nishimoto, N. Yokoyama, T. Sera, M. Suwa, Jpn. Tokyo Koho patent no. 78 138 992, 4 December 1978.
[16] Matsushita Electric Industrial Co. Ltd., Jpn. Tokyo Koho patent no. 58 124 544, 25 June 1983.
[17] Y. Ono, A. Nishino, Y. Takeuchi, H. Numamoto, Jpn. Tokyo Koho patent no. 60 220 149, 2 November 1985.
[18] B.K. Speronello, European patent no. 187 007, 9 July 1986.
[19] K. Byung-Hoon, N. Yong-Han, Ceram. Int. 21 (1995) 381–384.
[20] B.E. Yoldas, J. Mater. Sci., 23 (1988) 1895–1900.
[21] B.E. Yoldas, D.P. Partlow, J. Mater. Sci., 27 (1992) 6667–6672.
[22] A. Bachiorrini, G. Abbiati, Ceramurgia 3 (1983) 97–103.